Adsorption (2009) 15: 521–533
DOI 10.1007/s10450-009-9202-9

Sorbate densities on 5A zeolite above and below the critical conditions: *n* alkane data evaluation and modeling

Kevin F. Loughlin · Dana Abouelnasr

Received: 17 September 2009 / Accepted: 15 November 2009 / Published online: 25 November 2009

Abstract The sorbate densities of n-alkanes C_1–C_{20} in 5A zeolite are modeled. For validation of this model, the n-alkane adsorption data for gases and liquids on 5A zeolite is critically evaluated using the concept of sorbate densities. The adsorbed phase critical temperatures appear to occur at a reduced temperature of 0.975 different from the vapor-liquid critical reduced temperatures of 1.0 for C_3 to C_{20} n-alkanes. For methane and ethane species, the critical adsorbate reduced temperatures T_{CAR} occur earlier at reduced temperatures of 0.83 and 0.96 respectively. The modified Rackett equation of Spencer and Danner (1972) is satisfactorily used to calculate the adsorbate loading for $q_{\max}$ below adsorbed phase critical reduced temperature, T_{CAR}.

Above the critical adsorbate reduced temperatures, the saturated loading appears to be constant and equal to 8 ± 1 g/100 gZ for all the alkanes. The data in this region is scarce however, as there are not many isotherms above a T_{r} of 1.15. However the available isotherms appear to have a fairly equal and constant saturation loading between $T_{\mathrm{r}} = T_{\mathrm{CAR}}$ and $T_{\mathrm{r}} = 1.652$.

Keywords n-alkanes C_1–C_{20} · 5A zeolite · Sorbate densities · Sorbate molar volumes · Critical conditions

Nomenclature

a_0	saturation loading in Schirmer et al.'s paper (1968), mmol/g
b	van der Waals b, cc/mole
b_2	van der Waals b coefficient for a two phase system, cm^2/g
c	concentration of adsorbate in gas phase
l	linear slope for sorbate density decrease, Table 2
MW	molecular weight
n	number of carbon atoms in molecule
p	pressure, kPa
P_{c}	critical pressure, atm
P_{r}	reduced pressure
q	zeolite loading, g/100 gZ
$q_{\max}$	maximum zeolite loading, g/100 gZ
$q_{\max,\mathrm{c}}$	defined by (8)
$q^*_{\max}$	maximum adsorbent loading, g/100 g adsorbent
R	gas constant, 82.06 atm cc/gmol K
T_{b}	normal boiling point temperature, K
T_{c}	critical temperature, K
T_{CA}	critical temperature adsorbate, K
T_{CAR}	critical adsorbate reduced temperature
$T_{\mathrm{c}i}$	critical temperature, K, specie i
T_{r}	reduced temperature
$T_{\mathrm{r}i}$	mixture reduced temperature
u	power law factor for density, Table 2, Group 3
V_{A}	sorbate volume, cc/g or cc/mol
V_{c}	critical volume, cc/g
V_{sat}	saturated liquid volume, cc/g
w	power law factor for density, Table 2, Group 3
y_i	mole fraction
Z_{c}	critical compressibility
Z_{RA}	Rackett parameter

Greek Letters

β	molecular volume, Å^3/molecule

K.F. Loughlin (✉) · D. Abouelnasr
Department of Chemical Engineering, American University of Sharjah, PO Box 26666, University City, Sharjah, UAE
e-mail: kloughlin@aus.edu

D. Abouelnasr
e-mail: dabouelnasr@aus.edu

Γ normalized loading, dimensionless, calculated in (9)
ε_Z crystallographic 5A zeolite void volume, 0.47 cc/cc of zeolite (Breck 1974, page 133)
θ loading, at saturation $= 1$
ρ_{sat} sorbate liquid density, g adsorbate/cc
ρ_Z zeolite 5A crystallographic density, 1.99 g/cc (Breck 1974, page 133)
ω fraction of 5A zeolite crystals in the adsorbent
Ω sorbate density expansion parameter, Table 2, Group 2

1 Introduction

In a 1967 paper, Schirmer et al. (1968) stated that the limiting adsorption loading on 5A zeolite could be approximated for each n alkane using the volume of the zeolite cavity and the density of the liquid alkane under standard conditions This relation was limited to temperatures 50–100 K below the critical temperature, and was invalid in the region of the critical temperature. Since that time there has been an explosion in experimental measurements of n-alkane adsorption in 5A zeolite. The objective of this paper is to use the available data to investigate valid sorbate volume loadings covering the entire spectrum of temperatures above and below the critical temperature, and use them to validate an appropriate model of sorbate density.

2 Sorbate density or molar volume literature

In this study, the authors focused on sorbate densities for the limiting adsorption loading of n-alkanes in 5A zeolite crystals only. The limiting adsorption loading is defined to be the saturation loading where $\theta = 1$ as the fractional crystalline zeolite volume saturates. Consequently, our review of the literature focused primarily on this aspect. Data for gaseous adsorption isotherm studies and liquid saturation loadings of n-alkanes on 5A zeolite are abstracted from the literature. The relevant papers are tabulated in Table 1. The liquid saturation loadings are shown in italics in the Table. Data was obtained for all the n-alkanes C_1 to C_{14}, C_{16}, C_{18} and C_{20}. The emphasis was on gathering data near saturation loadings. Important gaseous studies were those of Schirmer et al. (1968), and Peterson and Redlich (1962) due to their diversity and that of Rolniak and Kobayashi (1980) due to the high reduced pressure and temperature used in measuring the methane isotherms. The most important liquid adsorption study was that of Sundstrom and Krautz (1968) as they measured the single component adsorption capacities for four n-alkanes, heptane, decane, dodecane and tetradecane at three different temperatures 30, 60 and 90 °C on two different batches of Linde type 5A molecular sieve pellets with 20% binder.

There are two problems in deciphering the literature on adsorption of n-alkanes in 5A zeolite. First, the adsorbent as reported in the various papers is in either crystalline 5A form

Table 1 n-alkane adsorption studies on 5A zeolite for gases and liquids. [Liquid loadings in italics]

Author	n-alkanes on 5A zeolite
Alkandary et al. (1995)	*dodecane, hexadecane and eicosane*
Doetsch et al. (1974)	heptane
Gupta et al. (1980)	*pentane, hexane, heptane and octane*
Jasra and Bhat (1987)	*octane, nonane, decane, undecane, dodecane, tridecane, tetradecane, hexadecane, octadecane*
Loughlin (1970)	methane, ethane propane & butane
Loughlin et al. (1990)	methane, propane, butane
Mentasty et al. (1991, 1994)	methane
Moeller et al. (2006)	butane, hexane
Miano (1996)	hexane, octane, decane, tetradecane, hexadecane
Nam et al. (2005)	methane, ethane
Pal et al. (1983)	heptane, dodecane
Peterson and Redlich (1962)	pentane, heptane, decane, hexadecane
Rolniak and Kobayashi (1980)	methane
Schirmer et al. (1968)	decane, undecane, dodecane, tridecane, tetradecane, octadecane
Silva and Rodriguez (1997a, 1997b)	hexane
Stroud et al. (1976)	methane
Sundstrom and Krautz (1968)	*heptane, decane, dodecane and tetradecane*
Vavlitis (1978)	pentane, octane, decane
Zuech et al. (1983)	methane

Table 2 Summary of various models to evaluate adsorbed phase volumes applicable to volumetric based adsorbents such as zeolites

Approximation for V_A	Temperature Range	Author
Group 1		
$V_A = V_S(T_b)$	All T	Rogers (1973)
		Findenegg (1984)
$V_A = V_S(T_b) + l(T - T_b)$	$T_b < T < T_c$	Dubinin (1960)
$= b$	$T > T_c$	
$l = (b - V_S(T_b))/(T_c - T_b)$		
$V_A = V_S(T)$	$T < T_c$	Mehta and Danner (1985)
$= V_S(T_c)$	$T > T_c$	
Group 2		
$V_A = V_S(T_b)\exp(\Omega(T - T_b))$	$T > T_b$	Ozawa et al. (1976)
$\Omega = 0.0025$		
$\Omega = \ln(b/V_S(T_b))/(T_c - T_b)$		Dubinin (1975)
Group 3		
$V_A = uT^w$	$T_b < T$	Cook and Basmadjian (1965)
u and w are parameters for tangent		
to ln V_S vs. ln T curve at T_b		

Note: b = van der Waals volume ($= V_C/3$ for the van der Waals equation of state)

only or pellets of 5A crystals with 20% binder [Linde 5A] or without binder [Grace]. It is assumed there is no adsorption of n-alkane on the binder. Many of the papers are imprecise in defining the experimental adsorbents used or whether their observed values for loadings were reported per gram of adsorbent or per gram of crystals. In these cases the authors deduced as best they could the material used. The second problem concerned capillary condensation of the n-alkanes in the pellets of 5A as saturation loading is approached. This was particularly evident in the methane on 5A gas adsorption studies of Mentasty et al. (1991, 1994) and in the liquid adsorption study of Gupta et al. (1980). A convex curve at the apex of the isotherms clearly indicates that the limiting adsorption loading of $\theta \rightarrow 1$ expressed on a crystal basis is being exceeded due to the capillary condensation in the small mesopores of the zeolite pellet. The problem was overcome by taking the last point on the concave downward portion of the isotherm as the limiting adsorption loading of $\theta \rightarrow 1$ expressed on a crystal basis.

There is a substantial literature on adsorbate molecular size to quantify the specific surface area of catalysts. This is generally concerned with small molecules such as nitrogen at its boiling point but the temperature dependence is in general not considered. As we are concerned primarily with the temperature dependence, this literature is not included in this survey.

Detailed literature on the variation of sorbate densities or molar volumes with temperature is primarily found in studies involving the adsorption potential isotherm on activated carbon. Comprehensive details are provided in the text by Tien (1994). More concise details are provided in the paper by Agarwal and Schwartz (1988).

The potential adsorption theory provides an initial means of examining the various methods used to model adsorbate densities. Agarwal and Schwartz (1988) summarize the models. They partition the methods used into three groups 1, 2 and 3. Group 1 models involve a linear variation of molar volume with temperature, group 2 models an exponential variation with temperature and group 3, models that cannot be categorized in either group 1 or 2. A summary of the groupings is presented in Table 2 for zeolites having a limited intrinsic pore volume. Three members of group 3 in the paper by Agarwal and Schwartz (1988) in Table 2 were omitted, as one is for a surface area based activated carbon and two other models were unsuccessful when applied generally (Lewis et al. 1950; Maslan et al. 1953).

The specific adsorbed phase volume in the first member of Group 1 is assumed to be constant equal to the specific volume at the boiling point for all T. However, the specific volume must increase with temperature, due to the greater rotational and vibrational energy of the molecules. This is consistent with the observed saturated adsorption amounts, which decrease with temperature. The product of the saturated adsorption amounts and the specific volume is representative of the adsorption space. Thus the product of a decreasing adsorption amount and constant specific volume implies a decreasing adsorption space; but this is not true as the adsorption space pore volume in zeolites is invariant with temperature. In the Multi Site Langmuir isotherm, both Silva and Rodriguez (1999) and Roma et al. (2005) used a constant specific adsorbate volume to calculate a fixed q_{max} of 13 g/100 g for 5A zeolite for C_3–nC_{10}, C_3 to nC_6, respectively. The temperature of a specific volume equivalent to a $q_{\max}$ of 13 g/100 g of zeolite is not specified presumably because it is temperature invariant. But, this raises the question of how it was first derived.

For the second member of group 1, the specific volume varies linearly with temperature between the specific volume at the normal boiling point temperature and van der Waals b at the critical point temperature. Above the critical temperature, the specific volume is assumed equal to b the van der Waals volume. The third member of group 1, a model proposed by Mehta and Danner (1985) uses the modified Rackett equation derived by Spencer and Danner (1972) to calculate the specific volumes below the critical temperature. However, the latter is not a linear variation with temperature but is a power law relationship. This implies that this method using Rackett's equation should really be a member of Group 3.

In Group 2, two methods assuming an exponential increase in V_{sat} with temperature are presented involving a volumetric expansion coefficient Ω. Expressions for the volumetric expansion coefficient are also included. Ozawa et al. (1976) selected the same expansion coefficient for all adsorbates whereas Dubinin (1960) employs different values for different adsorbates.

All methods that do not fit Groups 1 or 2 are placed in Group 3 with varying success. The method of Cook and Basmadjian (1965) involving a power law correlation of V_{sat} versus T estimated at the normal boiling may be applied to all temperatures above T_{b}. As already mentioned, the model of Mehta and Danner (1985) should probably be in this group as well.

Agarwal and Schwartz (1988) applied all the methods in the three groups to their data. They found that the three methods where V_{A} varied nonlinearly with temperature (Cook and Basmadjian 1965; Dubinin 1975; Ozawa et al. 1976) provided different but satisfactory results in representing their data for activated carbon adsorption.

In the above analysis for the potential theory isotherm, there is no discussion concerning the topic of critical temperature for an adsorbed phase, T_{CA}. In fact, it is assumed the same as the vapor-liquid system in all the studies above. De Boer (1968) discusses this topic in detail and indicates that the critical temperature for the adsorbed phase is much less than the critical temperature for the equivalent vapor-liquid system. Using van der Waals b for a three dimensional system equation of state, and an equivalent van der Waals b_2 for a two dimensional adsorbed phase equation of state, De Boer (1968) calculates that the two dimensional adsorbed phase critical temperature is related to the standard three dimensional critical temperature by the equation

$$T_{\mathrm{CA}} = 0.53 T_{\mathrm{c}}. \tag{1}$$

Thus it is substantially lower than for a vapor-liquid equilibrium system. For a zeolitic system involving both surface and microporous volume filling adsorption, such a large difference between the critical temperatures for the adsorbed phase and for the critical temperature for the vapor-liquid phase should not be anticipated as both surface forces and volume filling phenomena exist even though adsorption forces occupy the total force field. However we should expect it to be somewhat less than the vapor-liquid critical temperature.

Various isotherms have been used to characterize adsorption of n-alkanes on 5A zeolite. The Langmuir isotherm model gives saturation loadings varying with temperature, of which the papers by Moeller et al. (2006) and Miano (1996) are recent examples. The Ruthven isotherm has been used mainly to model the adsorption of methane on 5A zeolite (1971). The models for β the molecular volume of the adsorbed species in the Ruthven isotherm include equations for the variation of temperature above and below the critical conditions similar to the second member of group 1 in Table 2. Finally, the multisite Langmuir model was used by Silva and Rodriguez (1999) and by Roma et al. (2005) with an assumption that the adsorbate density is independent of temperature for C_3 to C_{10} alkanes. This is similar to the first member of group 1 in Table 2 but with V_{sat} chosen at an unspecified temperature.

3 Theoretical model

The theoretical saturation loading of n alkanes in 5A zeolite may be calculated from first principles for zeolite crystals and pellets of crystals and binder, assuming 100% accessibility for the alkanes (Do et al. 2009), as:

$$q_{\max}\left(\frac{\mathrm{g}}{100\ \mathrm{gZ}}\right) = 100\frac{\rho_{\mathrm{sat}}\varepsilon_{\mathrm{Z}}}{\rho_{Z}}. \tag{2}$$

For molecular sieves containing a fraction ω of crystal with a fraction of $(1-\omega)$ of binder, a factor of ω must be used to relate the reported loading based on adsorbent $q^{*}_{\max}$, to $q_{\max}$ based on crystals. For pure crystals, $\omega = 1.0$. For Linde 5A pellets, the fraction of binder in the pellets is generally stated as 20%. Hence, $\omega = 0.8$, and for these cases the saturation loading of an adsorbent is 80% of that for the pure crystals as expressed by (3).

$$q^{*}_{\max}\left(\frac{\mathrm{g}}{100\ \mathrm{g\ adsorbent}}\right) = q_{\max}\omega. \tag{3}$$

In these equations the saturation density for liquids below the critical point is calculated using the modified Rackett equation:

$$V_{\mathrm{sat}} = \frac{1}{\rho_{\mathrm{sat}}} = \left(\frac{\mathrm{RT_c}}{P_{\mathrm{c}}\mathrm{MW}}\right) Z_{\mathrm{RA}}^{\{1+(1-T_{\mathrm{r}})^{0.2857}\}} \tag{4}$$

Table 3 $q_{\max}$ calculated using (6) at various T_r's for 5A zeolite

Specie	$T_r = 0.7$	$T_r = 0.79$	$T_r = 0.9$	$T_r = 0.95$	$T_r = 0.975$	$T_r = 1$
	$q_{\max}$ g/100 g	$q_{\max}$ g/100 g	$q_{\max}$ g/100 g	$q_{\max}$ g/100 g	$q_{\max}$ g/100 g	$q_{\max,c}$ g/100 g
nC_1	9.16	8.32	7.23	6.44	5.86	3.80
nC_2	11.95	10.83	9.38	8.33	7.56	4.86
nC_3	12.94	11.71	10.12	8.98	8.14	5.20
nC_4	13.56	12.26	10.58	9.38	8.49	5.40
nC_5	13.92	12.57	10.83	9.58	8.66	5.48
nC_6	14.25	12.85	11.05	9.76	8.81	5.54
nC_7	14.39	12.97	11.13	9.82	8.86	5.54
nC_8	14.47	13.03	11.17	9.84	8.87	5.53
nC_{10}	14.68	13.19	11.28	9.91	8.92	5.51
nC_{11}	14.71	13.21	11.29	9.92	8.93	5.51
nC_{12}	14.64	13.14	11.21	9.84	8.84	5.43
nC_{14}	14.26	12.73	10.89	9.55	8.58	5.24
nC_{18}	15.68	12.78	11.81	10.29	8.57	5.49
nC_{20}	14.23	12.86	10.73	9.35	8.35	4.99
Average	14.30	13.01	11.00	9.67	8.71	5.39

Average is calculated for nC_3–nC_{20} in Table only

or the Rackett equation:

$$V_{\mathrm{sat}} = \frac{1}{\rho_{\mathrm{sat}}} = V_c Z_c^{(1-T_r)^{0.2857}}. \tag{5}$$

The modified Rackett equation is reported to be a ±2.4% improvement over the Rackett equation (Spencer and Danner 1972). However, in one instance the authors found the Rackett equation to be significantly better. Z_{RA} is a particular constant for the modified Rackett equation; values are given in the paper by Spencer and Danner (1972). In addition, values for all the critical constants and the Rackett parameter Z_{RA} are also given on the CHERIC website http://www.cheric.org/research/kdb/hcprop/cmpsrch.phpe.

Combining (2) and (4) gives the final equation for $q_{\max}$.

$$q_{\max}\left(\frac{\mathrm{g}}{100\ \mathrm{gZ}}\right) = 100\frac{\varepsilon_Z}{\rho_Z}\left(\frac{P_c\mathrm{MW}}{\mathrm{RT}_c}\right) Z_{\mathrm{RA}}^{-\{1+(1-T_r)^{0.2857}\}}. \tag{6}$$

An alternative expression is:

$$q_{\max}\left(\frac{\mathrm{g}}{100\ \mathrm{gZ}}\right) = q_{\max,c} Z_{\mathrm{RA}}^{-(1-T_r)^{0.2857}} \tag{7}$$

where $q_{\max,c}$ is the theoretical loading at critical vapor-liquid conditions:

$$q_{\max,c}\left(\frac{\mathrm{g}}{100\ \mathrm{gZ}}\right) = 100\frac{\varepsilon_Z}{\rho_Z}\left(\frac{P_c\mathrm{MW}}{\mathrm{RT}_c Z_{\mathrm{RA}}}\right). \tag{8}$$

Equation (7) may be rearranged to give a normalized value for the loading Γ by taking logarithms

$$\Gamma = -\frac{\log(q_{\max}/q_{\max,c})}{\log Z_{\mathrm{RA}}} = (1 - T_r)^{0.2857}. \tag{9}$$

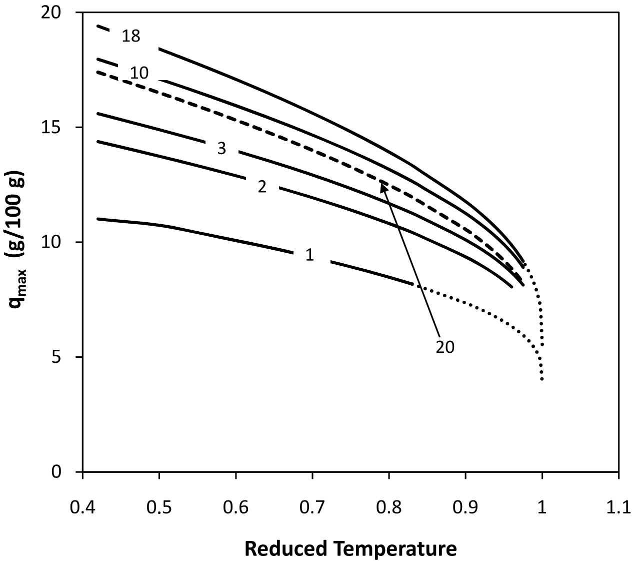

Fig. 1 Theoretical plot of $q_{\max}$ versus reduced temperature T_r calculated using (6) for *n*-alkanes ranging from C_1 to C_{20}. Curves are continued past the critical adsorbate temperature as dotted lines for C_1 and C_{18} only. Curve for C_{20} is shown as a *dashed line* for clarity

A theoretical plot of $q_{\max}$ versus reduced temperature T_r calculated using (6) is presented in Fig. 1 for several *n*-alkanes ranging from C_1 to C_{20}. Some important values are tabulated in Table 3. It was not possible to include all the *n*-alkanes on the plot due to merging of too many solid lines. The loading decreases monotonically with reduced temperature, and rapidly decreases as $T_r = 1$ is approached. This is a reflection of the increased rotational and vibrational energy of the molecules as the temperature increases. At any particular T_r, the loading increases monotonically as the carbon number increases up to a carbon number of C_{18} where a reversal occurs and a decrease is observed for C_{20}. The increase is quite marked for the C_1 to C_3 n-alkanes but then becomes much less significant as shown in Fig. 1 and in Table 3. For a T_r from approximately 0.3 to 0.975, the theoretical plot is shown as a solid line. The solid line is changed to a dotted line for the region where q_{max} falls below 8 g/100 gZ. The significance of this value will be discussed at a later point. The dotted line is shown only for C_1 and C_{18}. The other n-alkanes exhibit the same phenomenon also as is shown in Table 3. The q_{max} reduces by approximately a factor of 1.6 as the T_r region transits from 0.975 to 1.0. This reduction was not observed in the data which is why the line is shown dotted.

Theoretical values of q_{max} calculated using (6) are also presented in Table 3. Theoretical values are presented at T_r's of 0.7, 0.79, 0.9, 0.95, 0.975 and 1.0. The average value of q_{max} is also calculated for the C_3 to C_{20} listed n-alkanes and is shown in the bottom row. A T_r of 0.7 is taken to represent the normal boiling point so that the average value of 14.40 g/100 g represents a saturated liquid at this point. The T_r of 0.79 gives an average value of 13.01 which is the value used by Silva and Rodriguez (1999) and Roma et al. (2005) in the multisite Langmuir calculations for C_3 to C_{10} n-alkanes. However, the average value of q_{max} continues to decrease to 11 at a T_r of 0.9, 9.67 at a T_r of 0.95, 8.71 at a T_r of 0.975, rapidly decreasing to a average value of 5.39 at the critical point. This indicates that use of a constant value in any model may not give an appropriate representation of the true adsorption phenomena.

As will be shown, the minimum adsorption loading observed experimentally appears to be in the vicinity of 8 ± 1 g/100 gZ, so that use of ρ_{sat}'s calculated at a T_r greater than 0.975 is inappropriate for the C_3 to C_{20} n-alkanes. The T_{CAR}, the critical adsorbate reduced temperature, thus appears to be 0.975 for these n-alkanes. These results are consistent with those of Schirmer et al. (1968) who recommended that the appropriate calculation procedure for ρ_{sat} should be limited to 50 to 100 K below the critical temperature. Although methane and ethane are significantly different from all the other n alkanes because of their structure, the limitation of 8 ± 1 g/100 gZ also applies to both these molecules, but occurs at a lower temperature. Reviewing Table 3, the maximum applicable T_r for methane is found to be 0.83 and for ethane 0.96. Thus these are the critical adsorbate reduced temperatures T_{CAR} for these materials. Above these T_r values of 0.83 for methane and 0.96 for ethane, the maximum theoretical adsorption loading falls below 8 g/100 gZ, values not observed experimentally as will presently be seen. The calculation of the appropriate procedure to use above these T_r limiting values is discussed later.

3.1 Data evaluation

There are various ways of plotting experimental data of q versus p or c. The three standard methods are q versus p, ln q versus ln p, and q versus ln p. To determine the saturation loading from experimental data alone, we have found that the plot of q versus ln p gives the best representation of the data. The reason is that a full isotherm tends to have a complete italic S shape. If it does not reach this complete italic S shape, the isotherm is deemed unsaturated. This poses the question of how close to saturation are the observed isotherms? As we wanted to derive a model for sorbate densities which was independent of any model isotherm, we retained the values observed experimentally. This is similar to the procedure used by Schirmer et al. (1968). These values may be conservative and the true saturation values are likely to be somewhat higher than the last point.

The isotherms of methane on 5A zeolite are plotted in Fig. 2 for the data of Loughlin (1970), Loughlin et al. (1990), Zuech et al. (1983), and Rolniak and Kobayashi (1980). The data are shown as open circles or open squares and closed darkened squares. The closed darkened circles, all of which are from Rolniak and Kobayashi (1980), are adjudged to be close to saturation and the last value on these curves is assumed to be the saturated q_{max} at that temperature. The open circles are isotherms approaching saturation, but not as close, and open squares are far from saturation; these isotherms are eliminated from consideration in estimating the saturation q_{max}. In the case of methane isotherms in Fig. 2 the decision is clearcut. However, for some of the n-alkane isotherms for other species, the decision was not so clearcut. During the review of all the data, the authors adopted the following procedure. If both authors concurred, the isotherm was deemed close to saturation and designated with closed darkened circles; if only one author considered the isotherm saturated, the isotherm was given an opened circle symbol and adjudged to be not as close to saturation. Otherwise, the isotherm is given an open square. Obviously, less confidence may be placed in the open circles when they are presented in Figs. 8 to 11 than for the closed darkened circles in these Figures.

The authors abstracted and evaluated data on adsorption in 5A zeolite from 19 sources in the literature, and eventually plotted them as q_{max} versus reduced temperature T_r as in Figs. 6, 8–11. During the analysis procedure, the authors came across data that did not fit the general pattern in Figs. 6 to 11 causing these isotherms or data to be excluded from the Figures. The reasons for the exclusions include inconsistencies with other data, and different batches of 5A zeolite samples giving different results within the same study. Each exclusion is discussed.

Fig. 2 Summary of methane data on 5A zeolite. *Closed darkened circles* are isotherms close to saturation; *open circles* are isotherms approaching saturation but not as close; and *open squares* are far from saturation

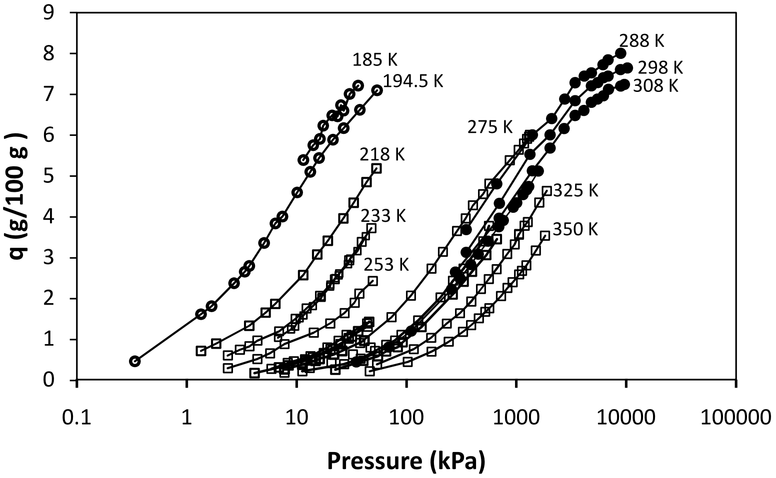

Fig. 3 Figure showing inconsistency of data from Nam et al. (2005) to data at similar temperatures from Rolniak and Kobayashi (1980), and Loughlin et al. (1990)

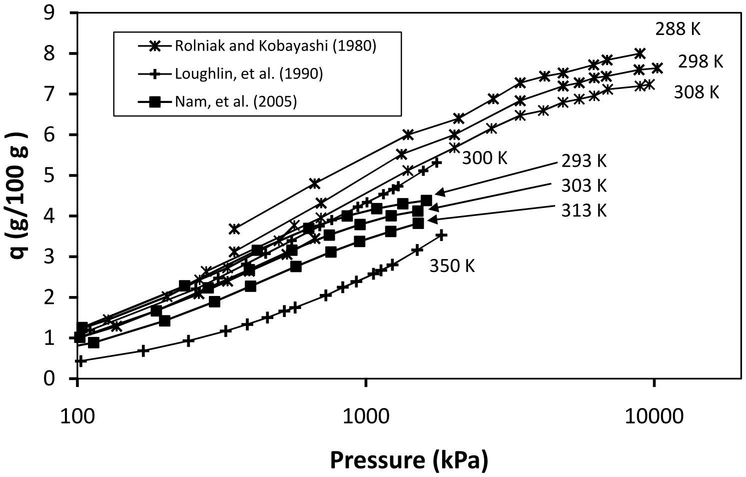

Data consistency was scrutinized first. The data of Nam et al. (2005) is plotted in Fig. 3 for the methane adsorption on 5A together with the data of Rolniak and Kobayashi (1980) and two isotherms of Loughlin et al. (1990); the latter data bracket the data of Nam et al. (2005). The data of Nam et al. (2005) illustrated with enclosed black squares is observed to be leveling off between 3 and 4 g/100 gZ. The other sets of data do not exhibit this phenomenon. In fact leveling off does not occur until a loading of approximately 7 to 8 g/100 gZ in the data of Rolniak and Kobayashi (1980). The Loughlin et al. (1990) data has not even reached the inflection point at 3 g/100 gZ. Accordingly, the data of Nam et al. for methane is excluded from all plots.

Pal et al. (1983), studied the sorption of *n*-heptane and *n*-dodecane on 5A. Their *n*-heptane data was found to be satisfactory and is included in the Figures. Their *n*-dodecane data is plotted with two isotherms of Schirmer et al. (1968) at 487.8 and 590.2 K in Fig. 4. The temperature of Pal et al.'s data ranges from 373 to 573 K. Their isotherms at 473 and 523 K are significantly lower than the isotherm of Schirmer et al. at 487 K. Further, Pal et al. have three isotherms at 473, 523 and 573 K below the isotherm of Schirmer et al. at 590 K. As the isotherms of Schirmer et al. are more con-

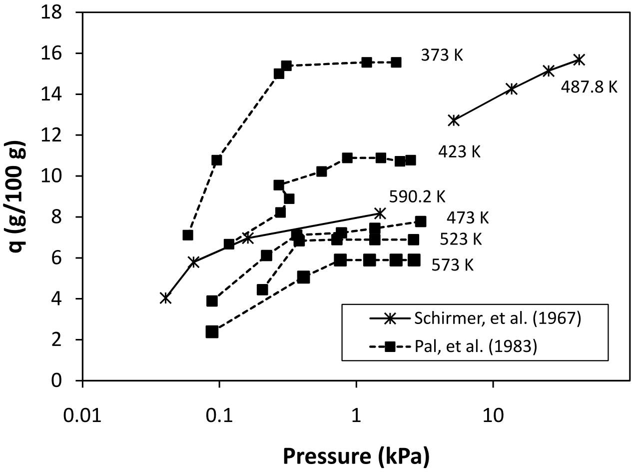

Fig. 4 Figure showing inconsistency of dodecane data on 5A zeolite from Pal et al. (1983) to data at similar temperatures from Schirmer et al. (1968)

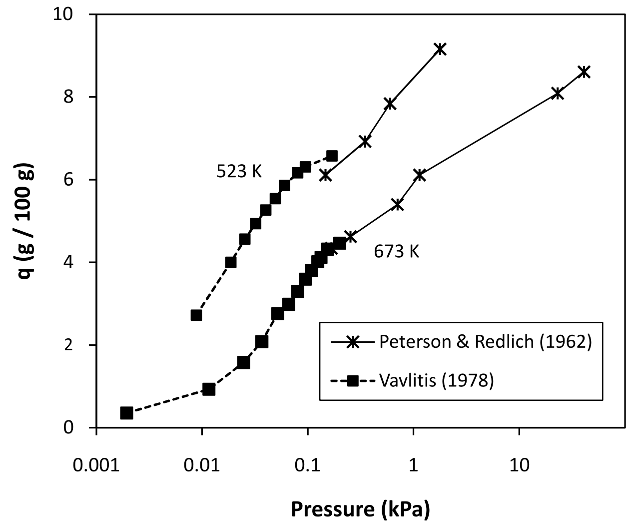

Fig. 5 Figure showing incompleteness of decane data on 5A zeolite from Vavlitis (1978) by comparison with data at the same temperatures from Peterson and Redlich (1962)

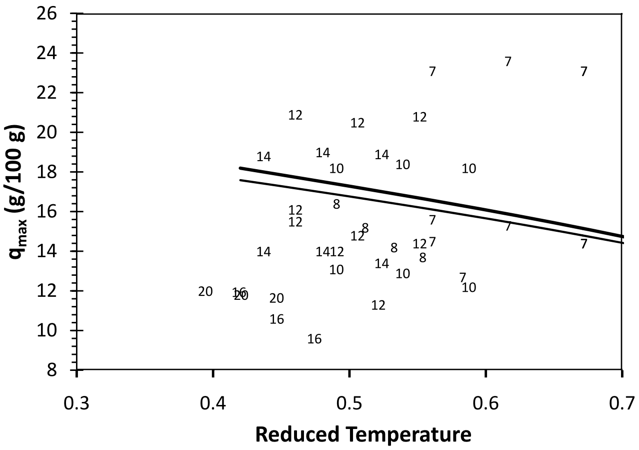

Fig. 6 Comparison of liquid $q_{\max}$ data on 5A zeolite with the theoretical model predictions of (6). Data numbers indicate relevant n-alkane species. Curves are for theoretical plot of $q_{\max}$ versus reduced temperature T_r calculated using (6) for C_{16} (*top curve*) and C_7 n-alkanes. Data of Sundstrom and Krautz (1968) [C_7, C_{10}, C_{12} & C_{14}], Alkandary et al. (1995) [C_8, C_{12}, C_{16} & C_{20}], Jasra and Bhat (1987) [C_8–C_{14}, C_{16} & C_{18}] and Gupta et al. (1980) [C_5, C_6, C_7 & C_8]

sistent with all the other data in the literature, in particular their saturation loadings, the dodecane isotherms of Pal et al. were excluded from any further consideration.

Analysis of the data of Vavlitis (1978), revealed that his hexane and octane data were satisfactory. The decane data was also thought to be satisfactory, until it was placed as open circles approaching saturation on Figs. 8 to 11. This produced a $q_{\max}$ loading that was extremely low in comparison to the other data. To validate the data, two similar isotherms at 523 and 673 K of Peterson and Redlich (1962) and Vavlitis (1978) are plotted on Fig. 5. Both sets of isotherms are continuous but with the Peterson and Redlich isotherms reaching much higher loadings, implying that the isotherms of Vavlitis are not near saturation. The reason why one of the authors concluded that the Vavlitis isotherms appeared to have leveled off at saturation may be observed by the top two points on these isotherms. Future investigators should be cautious when using these top two points. These two points illustrate the pitfalls confronting the authors when analyzing all the data in the literature, and in particular readers should be wary of the open circled saturation data.

The saturated liquid densities of Gupta et al. (1980), Alkandary et al. (1995), Sundstrom and Krautz (1968), and Jasra and Bhat (1987) are plotted in Fig. 6 together with the theoretical values calculated using (6). The results of this plot were a total surprise. Only the nC_7 data of Sundstrom and Krautz (1968), batch 1, was consistent with the theoretical plot. All the remaining data was significantly below the predicted values with the exception of the second batch of 5A zeolite used by Sundstrom et al. There are three possible explanations; either the system has not reached equilibrium, or the system has reached a pseudo-equilibrium, or the batches of 5A molecular sieve used were variable. Sundstrom et al. used two different batches of Linde 5A, one of which appears to greatly exceed the saturation loading as shown in the Fig. 6. The probable conclusion is that there is something amiss with this batch. This set of results was deemed infeasible and was removed from further consideration. The most probable explanation for the low $q_{\max}$ values is that these low temperature systems have reached a pseudo-equilibrium. Schirmer and coworkers (Academy of Sciences of the DDR 1979) established back in the 60's and 70's that an entropic effect arose in the diffusion of these higher n-alkanes. At high temperatures the entropy was such that the molecules diffused in as long chain molecules; as the temperature is lowered, the molecules ball up and sit in the cavity. If this happens, it is possible that only the outermost shells of the zeolites are occupied in the low temperature diffusion of the long chain alkanes, and that the inner core of the zeolite is relatively empty. This hypothesis can easily be tested by carrying out a study with smaller crystals such as Davison 5A. To sum up, it appears to be extremely difficult to measure accurate liquid loading data for the higher n-alkanes C_{10} to C_{20}.

3.2 Model Results

All the remaining darkened circled data for gaseous isotherms is plotted as $q_{\max}$ versus log P_r, for the various values of T_r at which the measurements were recorded for C_1 to C_{18} respectively in Fig. 7. The data for all the n-alkanes varies from a low reduced temperature T_r of 0.41 for hexadecane on the left hand side of the Figure (Peterson and Redlich) to a high reduced temperature of $T_r = 1.62$ for methane on

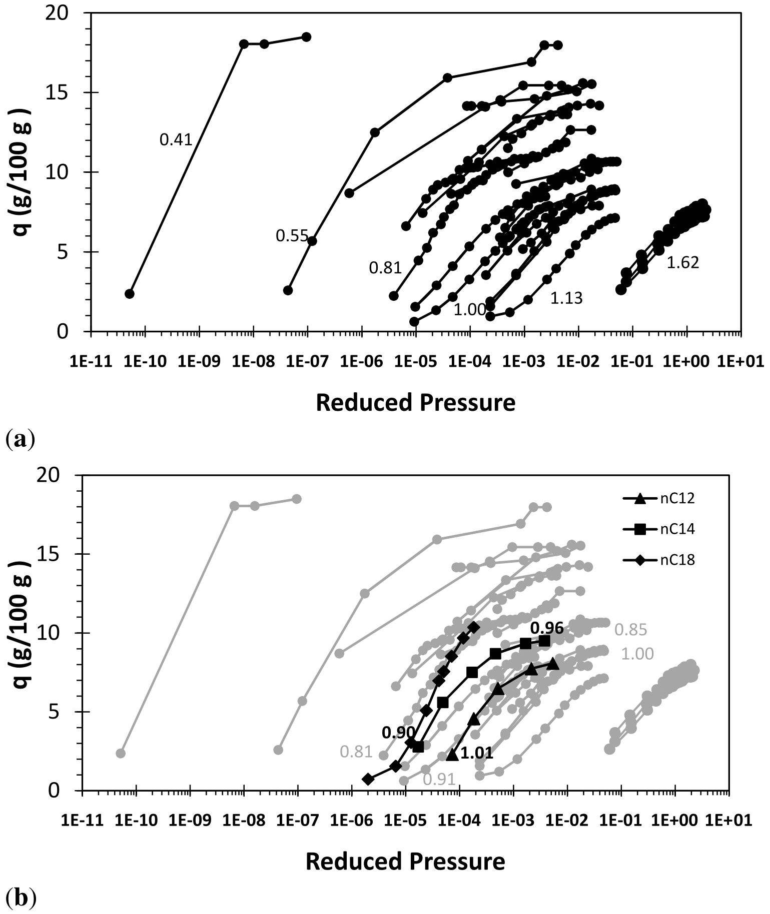

Fig. 7 (**a**) Selected isotherms for C_1 to C_{18} alkanes. Only saturated isotherms with a *closed darkened circle* are depicted. Numbers in Figure are reduced temperatures. (**b**) Figure showing displacement of C_{12}, C_{14} and C_{18} data of Schirmer et al. (1968) to the left on the diagram based on reduced temperatures. Background material is Figure (**a**). Three isotherms of Schirmer et al. (1967) are shown in the foreground

the right hand side (Rolniak and Kobayashi). The data is extremely extensive as there are 12 logarithmic decades of pressure on the abscissa axis. The data varies consistently following the expected progressive pattern of increasing P_r with increasing T_r for 15 n-alkanes, except for some data discussed in Fig. 7b. The data exhibits an empty L-shaped quarter at the top right hand corner of the Figure. The ordinate axis of this empty L-shaped quarter appears to occur at a reduced pressure of 0.03 for reduced temperatures below 1, at which stage the zeolites appear to be saturated with hydrocarbon. For practical applications, saturating adsorption columns do not need to exceed a reduced pressure of 0.03 for T_r's less than 1.00. For these conditions, it is not necessary to expend further energy compressing a gas to achieve saturation. At a low T_r of 0.55, the $q_{\max}$ loading is high at a saturation at about 18 g/100 gZ, demarcating the top ordinate of the L-shaped quarter. Increasing T_r's decrease the saturation loading reducing it to a value of about 8 ± 1 at high T_r's at the bottom ordinate of the L shaped quarter. The saturation then appears to remain constant with increasing T_r.

Figure 7a is reproduced as a grey background in Fig. 7b. Some of the data of Schirmer et al. (1968) for $n\mathrm{C}_{12}$, $n\mathrm{C}_{14}$, and $n\mathrm{C}_{18}$ is superimposed on the grey background of Fig. 7b. We originally placed all their data on the Figure but it became too confusing to explain. The data of Schirmer et al. for these alkanes exhibits the correct saturation loading but the isotherms appear to be translated towards the left hand ordinate-meaning a lower P_r than expected. For instance, the octadecane isotherm at $T_r = 0.90$ falls between the general T_r isotherms of 0.81 and 0.85. Similarly, the tetradecane isotherm of 0.96 falls below 0.85. The dodecane isotherm of 1.01 appears to fall on the general isotherm of 0.91. This was the general results observed for these three n-alkanes. As a consequence these isotherms are omitted from Fig. 7a. The authors are unable to explain this phenomenon and do not know whether it is an artifact or a true representation of the higher n-alkanes in general. However, the final saturation loadings were still used in the Figures that follow. It is important to note that the Schirmer et al. (1968) isotherms for C_{10} and C_{11} fit satisfactorily into Fig. 7a. So it is only the translation of the higher n-alkanes that is unusual.

The saturation end points of the isotherms, $q_{\max}$, were plotted versus reduced temperature for all the n-alkanes together with theoretical values calculated using (6). Three typical plots are shown in Fig. 8 for $n\mathrm{C}_4$, $n\mathrm{C}_7$ and $n\mathrm{C}_{18}$. The solid theoretical lines shown on the Figures are for calculations of $q_{\max}$ using sorbate density derived from (6). The

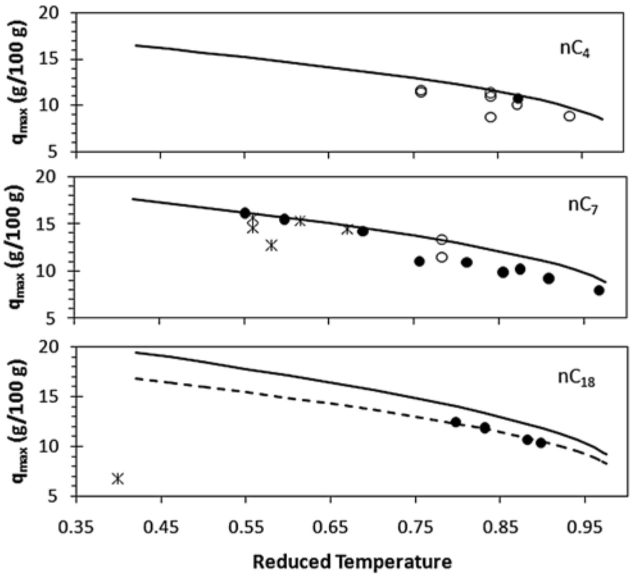

Fig. 8 Fit of (6) to experimental data of nC_4, nC_7 and nC_{18}. *Closed darkened circles* are for gaseous saturation isotherms. *Open circles* are for gaseous isotherms approaching saturation but not as close. *Stars* are for liquid data. The *solid line* indicates (6). The *dashed line* indicates (2) with the Rackett's equation

dotted line for nC_{18} is for $q_{\max}$ calculated using the Rackett's equation (5) to estimate density rather than the modified Rackett's equation. For nC_4 and nC_7, there was no difference between using the Rackett equation or the modified Rackett equation to calculate $q_{\max}$. For nC_{18} the Rackett equation model is shown as a dashed line. In addition to the closed and opened circle data mentioned earlier, the liquid saturation density data of Sundstrom et al. for nC_7 and of Jasra and Bhat (1987) for nC_{18} is included as star symbols. Further, since the data are from isotherms which may not be quite at saturation conditions, values may reside below the theoretical plots. The fit of (6) to the experimental data is excellent for nC_4 and nC_7 including the liquid experimental data. For nC_{18}, the theoretical model using Racketts equation as the calculation method for density gives an excellent fit to the experimental data. However, the liquid data point of Jasra and Bhat (1987) is extremely low indicating the difficulty of measuring liquid loadings for these large n-alkanes. All the other n-alkanes exhibited similar excellent fits for theory and experiment.

The data at temperatures below the critical adsorbate reduced temperature may be fitted with a normalized modified Rackett curve Γ as in (9). The left hand side of (9), Γ, is plotted against T_r in Fig. 9. The theoretical saturations for all n-alkanes are now collinear and are shown as a solid line. The normalized experimental saturation loadings mostly fall below the theoretical plot. This is consistent with the model as the isotherms from which they are taken may be only approaching saturation. The liquid saturation data is significantly worse than the enclosed circle data as is expected.

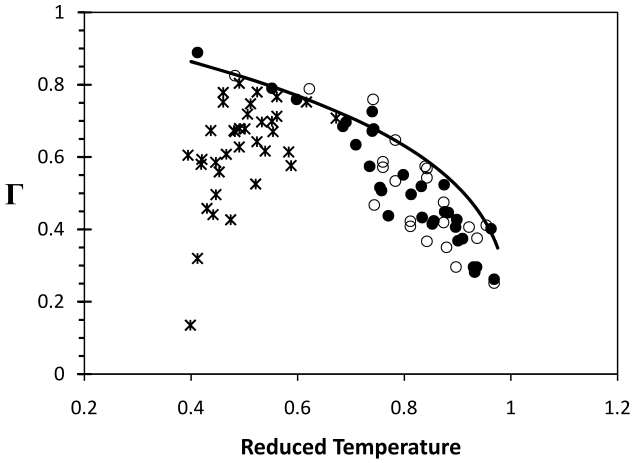

Fig. 9 *Solid line* is the theoretical plot of normalized parameter Γ—(9)—against reduced temperature. *Closed darkened circles* are for gaseous saturation isotherms. *Open circles* are for gaseous isotherms approaching saturation but not as close. *Stars* are for liquid data

The fit of the $q_{\max}$ experimental data to the theoretical model given by (6) indicates that the critical adsorbate reduced temperature in the adsorbed phase is not at $T_r = 1$ but rather at $T_r \approx 0.975$ for the C_3 to C_{18} n-alkanes; for a T_r between 0.975 and 1.0, the model in this region indicates that the sorbate volume calculated using (6) should be halved which is not consistent with experimental data. Similar observations apply to the lower T_{CAR} for methane and ethane. This observation that the adsorbed phase critical temperature is less than the vapor-liquid phase critical temperature is consistent with the work of De Boer (1968). However, the difference between the adsorbed phase and vapor-liquid phase critical temperatures is not as large as he observed.

Schirmer et al. (1968) tabulated the saturation loadings a_0 in their paper in mmol/gZ for C_3 to C_{18} n-alkanes. These values and the temperatures at which they are reported are tabulated in Table 4. These a_0 values are recalculated in column 5 in the Table as $q_{\max}$ values in g/100 g. Also tabulated are the $q_{\max}$ values estimated using (6) as g/100 g in column 6. The observed values from Schirmer et al. are in excellent agreement with the model values. The caveat of Schirmer et al. (1968) that this comparison of theory and experiment should only be applied 50 to 100 K below the critical temperature can be relaxed somewhat. $q_{\max}$ calculated by (6) for the isothermal data appears to be valid up to a T_r of 0.975 which is only 10 to 20 K below the critical temperature.

The adsorbed phase above the critical reduced temperature of the adsorbate appears to level off at a uniform value of $q_{\max}$ as is plotted in Fig. 10. The first observation to note is that these values are substantially greater than the average value of 5.39 tabulated in Table 3 for the critical point. Hence it is clear that the reduced temperature critical point for the adsorbed phase has been lowered and the data appears to indicate that it is in the vicinity of $T_r = 0.975$ for

Table 4 Limiting adsorption loadings of n-alkanes by 5A zeolite (data of Schirmer et al. 1968)

n alkanes	T in K	T_r	a_0 mmol/gZ	q_{max} g/gZ	q_{max} by Rackett's Eq g/gZ
nC3	298	0.805776	3.09	13.62573	11.63
nC4	298	0.701176	2.25	13.07768	13.55
nC5	298	0.634448	1.95	14.06921	14.69
nC6	298	0.587076	1.63	14.04679	15.60
nC10	457	0.739841	0.98	13.94383	14.12
nC11	473	0.740219	0.97	15.16217	14.14
nC12	487	0.740122	0.92	15.671	14.07
nC13	509	0.754074	0.58	10.69288	13.44
nC14	533	0.76912	0.51	10.11794	13.27
nC18	595	0.796519	0.5	12.7249	14.04

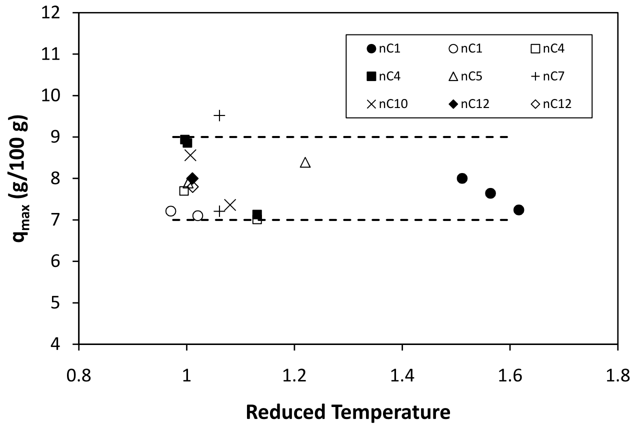

Fig. 10 Plot of the available q_{max} data above the adsorbate critical temperature. Also shown are the outer limits for the predicted saturated loadings in (10)

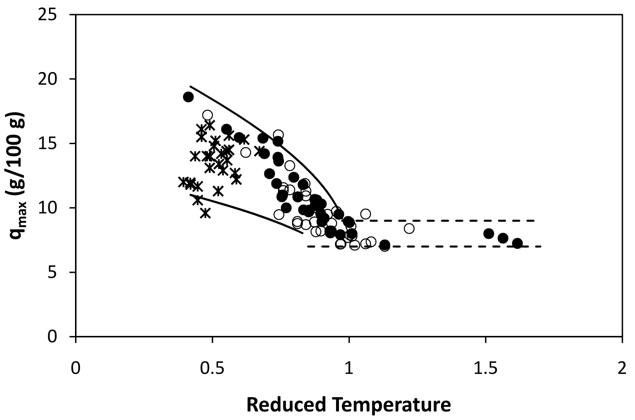

Fig. 11 Summary of all q_{max} data for n-alkanes versus T_r. Equation (6) is plotted for nC_1 and nC_{18} for T_r below the critical adsorbate temperature. Above the critical adsorbate temperature the data is bounded by (10)

the n-alkanes greater than C_3. There is a significant scatter in the data in Fig. 10 and the authors are unable to say whether a trend exists. The q_{max} values range from 7.01 to 9.52, have a mean value of 7.86, a standard deviation of 0.73 and a standard error of 0.35. To encompass all the data except one point, the authors recommend using 8 ± 1 as the predicted theoretical value. We recommend that these values be used as the appropriate theoretical calculation procedure for all T_r's above 0.975 for n-alkanes C_3 and higher. The same equation should be applied to C_1 and C_2 but starting at a T_r of 0.83 and 0.96 respectively. The authors make a strong plea for a definitive study of the sorbate densities in this region for various T_r's and for various n alkanes.

The experimental data and model theoretical fits are plotted in Fig. 11. For the model theoretical plots for T_r less than 0.975, only the curves for C_1 and C_{18} are shown as adding more predictive curves makes the Figure too congested. Although all the experimental data in this region seems to fall neatly between these two curves, only the upper bound of C_{18} has a physical significance. All the experimental data should fall on or below the upper bound. The fact that most of the experimental data falls above the lower bound C_1 is fortuitous and has no physical significance. The experimental data above $T_r = 0.975$ exhibits some scatter but the theoretical plot with the bounds encloses all but one of the data points.

Consequently, the sorbate densities may be theoretically evaluated using (6) below the critical adsorbate reduced temperatures for:

methane	$T_{CAR} = 0.83$
ethane	$T_{CAR} = 0.96$
all other n-alkanes	$T_{CAR} = 0.975$

Above the critical adsorbate reduced temperatures, the equation to use is (10):

$$q_{max} = 8.0 \pm 1.0 \frac{\text{g}}{100\ \text{gZ}}. \tag{10}$$

The model proposed is similar to the third member of group 1 in Table 2 proposed by Mehta and Danner (1985).

The similarities are that the liquid density is calculated using (6) up to the appropriate T_{CAR}. The differences are that the critical adsorbate reduced temperatures T_{CAR} appears to be 0.83, 0.96 and 0.975 for the relevant n-alkanes rather than at a T_c of 1. Secondly, the sorbate density for $T_r > T_{\mathrm{CAR}}$ is not the value at the critical point T_c but rather $= 8 \pm 1$ g/100 gZ which is approximately 1.6 times the value at T_c. As already mentioned, this model should probably be placed in group 3 in Table 2 as it is nonlinear.

3.3 Thermodynamic consistency test

To maintain thermodynamic consistency, the multi-site Langmuir model of Nitta et al. (1984) requires that

$$\frac{nq_{\max}}{\mathrm{MW}} = \text{constant}. \tag{11}$$

An alternative way to state this is that the number of CH_2–units on saturation does not vary with n at a given temperature. This may be one of the reasons why Silva and Rodriguez (1999) chose a fixed $q_{\max}$ for n-alkanes propane to decane. However, thermodynamic consistency may still be achieved by choosing an appropriate T_r for an adsorption mixture entering an adsorption column. Table 3 indicates that when T_r is fixed the value of $q_{\max}$ is fairly constant for the propane to hexadecane hydrocarbons but in general different from 13 g/100 g zeolite. A mixture T_r may be selected using an appropriate equation such as

$$T_r = \sum_{i=1}^{n} y_i T_{ri} \tag{12}$$

where

$$T_{ri} = \frac{T}{T_{ci}}. \tag{13}$$

4 Conclusions

The sorbate molar volume of n-alkanes C_1–C_{18} in 5A zeolite is modeled and validated using the completed italic S isotherms of each species as experimental data. The conclusion of Schirmer et al. (1968) that the isotherm data below the critical temperature may be modeled accurately using a suitable saturated liquid density equation is vindicated up to a T_r of approximately 0.83, 0.96 or 0.975 for methane, ethane and C_3 to C_{18} n-alkanes. The critical adsorbate phase temperatures appear to be different from the vapor-liquid critical temperatures as documented by De Boer (1968). The modified Rackett equation of Spencer and Danner (1972) may be satisfactorily used to calculate the adsorbate loading in this region.

Above a T_r of approximately 0.975, the saturated loading appears to be constant and equal to 8 ± 1 g/100 gZ. The data in this region is scarce however; but the limited data appears constant in the region between $T_r = 0.975$ and $T_r = 1.652$. Schirmer et al. (1968) provided no equation in this region for comparison purposes.

Acknowledgements This is a detailed paper of a poster paper presented at PBAST 5, May 24–26, 2009, Singapore. The authors wish to acknowledge the support of the American University of Sharjah during the execution of this study. This full paper has been accepted for presentation in FOA10 at Kyoto, Japan, 2010.

References

Academy of Sciences of the DDR: Adsorption of Hydrocarbons in Zeolites, vol. 1 & 2. Preprints of the Workshop, November 19–22, Berlin GDR (1979)

Agarwal, R.K., Schwartz, J.A.: Analysis of high pressure adsorption of gases on activated carbon by potential theory. Carbon **26**(6), 873–887 (1988)

Alkandary, J.A.M., Al-Ammeri, R., Salem, A.B.S.H.: Adsorption equilibria of normal paraffins on 5A molecular sieve. Sep. Sci. Technol. **30**(16), 3195–3209 (1995)

De Boer, J.H.: The Dynamical Character of Adsorption, 2nd edn. Oxford University Press, London (1968)

Breck, D.W.: Zeolite Molecular Sieves. Wiley, New York (1974)

Cook, W.H., Basmadjian, D.: The prediction of binary adsorption equilibriums from pure component isotherms. Can. J. Chem. Eng. **43**(2), 78–83 (1965)

Doetsch, I.H., Ruthven, D.M., Loughlin, K.F.: Sorption and diffusion of n-heptane in 5A zeolite. Can. J. Chem. **52**(15), 2717–2724 (1974)

Do, D.D., Do, H.D., Nicholson, D., Herrera, L., Wongkoblap, A.: The role of accessibility in the characterization of porous solids and their adsorption properties. In: PBAST 5, May 24–27, Singapore (2009)

Dubinin, M.M.: The potential theory of adsorption of gases and vapors for adsorbents with energetically non-uniform surfaces. Chem. Rev. **60**, 235–241 (1960)

Dubinin, M.M.: Physical adsorption of gases and vapors in micropores. In: Cadenhead, D.A., et al. (eds.) Prog. Surf. and Membrane Science, vol. 9, pp. 1–70. Academic Press, New York (1975)

Findenegg, G.: High pressure physical adsorption of gases on homogeneous surfaces. In: Myers, A.L., Belfort, G. (eds.) Fundamentals of Adsorption, pp. 207–218. Engineering Foundation, New York (1984)

Gupta, R.K., Kunzru, D., Saraf, D.N.: Liquid Phase Adsorption of n-paraffins on molecular sieve. J. Chem. Eng. Data **25**, 14–18 (1980)

Jasra, R.V., Bhat, S.G.T.: Thermal desorption of normal paraffins from zeolite 5A. Zeolites **7**(3), 127–130 (1987)

Lewis, W.K., Gilliland, E.R., Chertow, B., Cadogan, W.P.: Adsorption equilibria. Hydrocarbon gas mixtures. J. Ind. Eng. Chem. **42**, 1319–1326 (1950)

Loughlin, K.F.: Sorption in 5A zeolite. Ph.D. Thesis, University of New Brunswick, Fredericton, NB, Canada (1970)

Loughlin, K.F., Hasanain, M.A., Abdul_Rehman, H.: Quaternary, ternary, binary, and pure component sorption on zeolites. 2. Light alkanes on Linde 5A and 13X zeolites at moderate to high pressures. Ind. Eng. Chem. Res. **29**(7), 1535–1546 (1990)

Maslan, F.D., Altman, M., Albert, E.R.: Prediction of gas adsorbent equilibria. J. Phys. Chem. **57**, 106–109 (1953)

Mehta, S.D., Danner, R.P.: An improved potential theory method for predicting gas adsorption equilibria. Ind. Eng. Chem. Fund. **24**(3), 325–330 (1985)

Mentasty, L., Faccio, R.I., Zgrablich, G.: High Pressure methane adsorption in 5A zeolite and the nature of the gas solid interactions. Adsorpt. Sci. Technol. **8**(2), 105–113 (1991)

Mentasty, L., Woestyn, A., Zgrablich, G.: High pressure methane adsorption on natural and synthetic zeolites. Adsorpt. Sci. Technol. **11**(2), 123–133 (1994)

Miano, F.: Adsorption of hydrocarbon vapor mixtures onto zeolite 5A. Colloids Surf. A, Physiochem. Eng. Asp. **110**, 95–104 (1996)

Moeller, A., Yang, X., Caro, J., Staudt, R.: Measurement of the adsorption of n-alkanes in 5A zeolite. Chem. Ing. Tech. **78**(12), 1831–1836 (2006)

Nam, G.-M., Jeong, B.M., Kang, S.-H., Lee, B.-K., Choi, D.-K.: Equilibrium isotherms of CH_4, C_2H_6, C_2H_4, N_2 and H_2 on zeolite 5A using a static volumetric method. J. Chem. Eng. Data **50**(1), 72–76 (2005)

Nitta, T., Shigetomi, T., Kuro-Oka, M., Katayama, T.: An adsorption isotherm of multi-site occupancy model for homogeneous surfaces. J. Chem. Eng. Jpn. **17**, 39–45 (1984)

Ozawa, S., Kusumi, S., Ogino, Y.: Physical adsorption of gases at high pressure. IV. An improvement of the Dubinin-Astakhov adsorption equation. J. Colloid Interface Sci. **56**(1), 83–91 (1976)

Pal, T.K., Roessch, J., Fetting, F., Mukherjee, R.N.: Investigations of adsorption of n-heptane, n-dodecane, and their mixtures on 5A molecular sieves. Ger. Chem. Eng. **6**, 371–381 (1983)

Peterson, D.L., Redlich, O.: Sorption of normal paraffins by molecular sieves type 5A. J. Chem. Eng. Data **7**(2), 570–574 (1962)

Rogers, K.A.: Adsorption on activated carbon by hydrogen, methane and carbon dioxide gases and their mixtures at 212.deg.K to 301.deg.K and up tp 35 atmospheres. Ph.D. Thesis, Georgia Institute of Technology, Atlanta, GA (1973)

Rolniak, P.D., Kobayashi, R.: Adsorption of methane and several mixtures of methane and carbon dioxide at elevated pressures and near ambient temperatures on 5A and 13X molecular sieves by tracer perturbation chromatography. AIChE J. **26**(4), 616–624 (1980)

Roma, F., Ricardo, J.L., Ramirez-Pastor, A.J.: Statistical thermodynamic models for polyatomic adsorbates; application to adsorption of n-paraffins in 5A zeolite. Langmuir **21**(6), 2454–2459 (2005)

Ruthven, D.M.: Simple theoretical adsorption isotherm for zeolites. Nat. Phys. Sci. **232**(29), 70–71 (1971)

Schirmer, W., Fiedrich, G., Grossmann, A., Stach, H.: Adsorption behaviour of pure and mixed n-alkanes of medium chain length on zeolites. In: Molecular Sieves: Papers read at the conference held at the School of Pharmacy, University of London, 4–6 April, 1967, pp. 276–290. London Society of Chemical, Industry (1968)

Silva, J.A., Rodriguez, A.E.: Sorption and diffusion of n-pentane in pellets of 5A zeolite. Ind. Eng. Chem. Res. **36**, 493–500 (1997a)

Silva, J.A., Rodriguez, A.E.: Equilibrium and kinetics of n-hexane sorption in pellets of 5A zeolite. AIChE J. **43**, 2524–2534 (1997b)

Silva, J.A., Rodriguez, A.E.: Multi-site Langmuir model applied to the interpretation of sorption of n-paraffins in 5A zeolite. Ind. Eng. Chem. Res. **38**, 2434–2438 (1999)

Spencer, C.T., Danner, R.P.: Improved equation for prediction of saturated liquid density. J. Chem. Eng. Data **17**(2), 236–240 (1972)

Stroud, H.J.F., Richards, E., Limchareon, P., Parsonage, N.G.: Thermodynamic study of the Linde 5A + methane system. J. Chem. Soc. Faraday Trans. I **72**(4), 942–954 (1976)

Sundstrom, D.W., Krautz, F.G.: Equilibrium adsorption of liquid phase normal paraffins on type 5A molecular sieves. J. Chem. Eng. Data **13**(2), 223–226 (1968)

Tien, C.: Adsorption Calculations and Modeling. Butterworth Heinemann, Boston (1994)

Vavlitis, A.P.: Adsorption kinetics in 5A and 13X zeolites. MS Thesis, University of New Brunswick, Fredericton, Canada (1978)

Zuech, J.I., Hines, A.L., Sloan, E.D.: Methane adsorption on 5A molecular sieve in the pressure range 4 to 690 kPa. Ind. Eng. Chem. Process. Des. Dev. **22**, 172–174 (1983)